

Cyanidin-3-glucoside, a Natural Product Derived from Blackberry, Exhibits Chemopreventive and Chemotherapeutic Activity*

Received for publication, January 27, 2006, and in revised form, March 30, 2006. Published, JBC Papers in Press, April 17, 2006, DOI 10.1074/jbc.M600861200

Min Ding^{†1}, Rentian Feng[‡], Shioh Y. Wang[§], Linda Bowman[‡], Yongju Lu[‡], Yong Qian[‡], Vincent Castranova[‡], Bing-Hua Jiang[¶], and Xianglin Shi[‡]

From the [†]Pathology and Physiology Research Branch, Health Effects Laboratory Division, National Institute for Occupational Safety and Health, Morgantown, West Virginia 26505, the [§]Fruit Laboratory, Beltsville Agricultural Research Center, U. S. Department of Agriculture, Beltsville, Maryland 20705, and the [¶]Department of Microbiology, Immunology, and Cell Biology, West Virginia University, Morgantown, West Virginia 26505

Epidemiological data suggest that consumption of fruits and vegetables has been associated with a lower incidence of cancer. Cyanidin-3-glucoside (C3G), a compound found in blackberry and other food products, was shown to possess chemopreventive and chemotherapeutic activity in the present study. In cultured JB6 cells, C3G was able to scavenge ultraviolet B-induced $\cdot\text{OH}$ and O_2^- radicals. *In vivo* studies indicated that C3G treatment decreased the number of non-malignant and malignant skin tumors per mouse induced by 12-*O*-tetradecanoylphorbol-13-acetate (TPA) in 7,12-dimethylbenz[*a*]anthracene-initiated mouse skin. Pretreatment of JB6 cells with C3G inhibited UVB- and TPA-induced transactivation of NF- κ B and AP-1 and expression of cyclooxygenase-2 and tumor necrosis factor- α . These inhibitory effects appear to be mediated through the inhibition of MAPK activity. C3G also blocked TPA-induced neoplastic transformation in JB6 cells. In addition, C3G inhibited proliferation of a human lung carcinoma cell line, A549. Animal studies showed that C3G reduced the size of A549 tumor xenograft growth and significantly inhibited metastasis in nude mice. Mechanistic studies indicated that C3G inhibited migration and invasion of A549 tumor cells. These findings demonstrate for the first time that a purified compound of anthocyanin inhibits tumor promoter-induced carcinogenesis and tumor metastasis *in vivo*.

Chemoprevention, the use of drugs or natural substances to retard or reverse the process of carcinogenesis, represents one of several promising strategies to reduce the development of cancer. Many naturally occurring substances present in the human diet have been identified as potential chemopreventive and/or chemotherapeutic agents (1–3). A recent report published by the American Institute for Cancer Research regarding dietary prevention of cancer indicates that ~7–31% of all cancers worldwide could be reduced by diets high in fruits and vegetables (4, 5). Thus, searching for novel natural agents and defining novel targets for chemoprevention have become intense areas of investigation.

A recent study demonstrated that topical application of plant-derived chemicals, such as caffeine or (–)-epigallocatechin gallate, inhibits carcinogenesis and selectively increases apoptosis in UVB²-treated mouse

skin (6). Our previous study also indicated that fresh apple peel extract exhibits anticarcinogenesis activity (7).

In a search for better chemopreventive or chemotherapeutic agents, we isolated cyanidin-3-glucoside (C3G) from blackberries (8). C3G belongs to the flavonoid class of molecules and is a member of the anthocyanin family, the largest group of pigments present in many edible berries, dark grapes, cabbages, and other pigmented foods. Evidence suggests that anthocyanins may serve as natural antioxidants (9). Anthocyanins repair and protect genomic DNA integrity. Studies have shown that berry anthocyanins are beneficial in reducing age-associated oxidative stress, as well as in improving neuronal and cognitive brain function. Early studies have shown that supplementations with berries rich in anthocyanins were effective in reducing oxidative stress associated with aging, and were beneficial in reversing age-related neuronal and behavioral changes (9, 10).

Over the past decades, extensive efforts have been made to develop targeted therapies that can inhibit or prevent tumorigenesis. In this regard, AP-1, NF- κ B, MAPKs, COX-2, and TNF α represent the most promising pharmacological targets that have been identified (7, 11–13). Activation of those targets/pathways has been shown to be involved in tumor growth and development (14–16).

Previous studies have reported that both AP-1 and NF- κ B are known to be involved in transcriptional regulation of matrix metalloproteinase, angiogenic enzymes that play an important role in malignant cancer cells invasion and metastasis (17). AP-1 and NF- κ B also up-regulate the expression of urokinase-type plasminogen activator (uPA) and its receptor (uPAR). The inhibition of NF- κ B and AP-1 suppressed the secretion of uPA, resulting in the inhibition of motility of highly invasive breast cancer cells (18). Increased AP-1 activity is associated with malignant transformation and the action of cancer-promoting agents (15, 16). Blocking TPA-induced AP-1 activation has been shown to inhibit neoplastic transformation (19). Moreover, a recent study using transgenic mice has demonstrated that AP-1 transactivation is required for tumor promotion (20).

COX-2 and TNF α are also important targets for modulating inflammation and carcinogenesis. TNF α inhibitors display a significant effect in retarding inflammatory disease and carcinogenesis (21). COX-2, a

* The costs of publication of this article were defrayed in part by the payment of page charges. This article must therefore be hereby marked "advertisement" in accordance with 18 U.S.C. Section 1734 solely to indicate this fact.

¹ To whom correspondence should be addressed: Pathology and Physiology Research Branch, Health Effect Laboratory Division, National Institute for Occupational Safety and Health, 1095 Willowdale Road, Morgantown, WV 26505. Tel.: 304-285-6229; Fax: 304-285-5938; E-mail: mid5@cdc.gov.

² The abbreviations used are: UVB, ultraviolet B; C3G, cyanidin-3-glucoside; DMBA, 7,12-

dimethylbenz[*a*]anthracene; AP-1, activator protein-1; COX-2, cyclooxygenase-2; TNF α , tumor necrosis factor α ; NF- κ B, nuclear factor κ B; MAPK, mitogen-activated protein kinase; MAPKK, MAPK kinase; ERK, extracellular signal-regulated kinase; JNK, c-Jun N-terminal kinase; MKK4, MAP kinase kinase 4 (alternatively designated SEK1 or MEK4); TPA, 12-*O*-tetradecanoylphorbol-13-acetate; FBS, fetal bovine serum; ROS, reactive oxygen species; uPA, urokinase-type plasminogen activator; uPAR, urokinase-type plasminogen activator receptor; CM-DCFDA, carboxymethyl dichlorofluorescein diacetate; PBS, phosphate-buffered saline; ABTS, 2,2'-azobis(2-amidinopropane) dihydrochloride.

Chemopreventive and Chemotherapeutic Effects of C3G

catalyst in prostaglandin synthesis from arachidonic acid, contributes to the regulation of angiogenesis and metastasis (22, 23). Selective COX-2 inhibitors protect against the formation of tumors in animals, suggesting that prostaglandins, the products of COX-2 activity, substantially contribute to carcinogenesis (24–26). Overexpression of COX-2 is common in human lung cancer and seems to be associated with tumor progression, invasion, and metastasis. In experimental animal models, COX-2 has been shown to be involved in tumor angiogenesis, suggesting that COX-2 is a potential target for cancer therapy. Several *in vivo* studies have already shown that COX-2-specific inhibitors (celecoxib and rofecoxib) have antitumor activity, and clinical trials using COX-2 inhibitors are currently ongoing in patients with lung cancer (27, 28).

Reports focusing on mechanisms and *in vivo* data supporting the possible chemopreventive and chemotherapeutic effects of purified C3G are limited. In light of the important roles of NF- κ B, AP-1, COX-2, TNF α , and MAPK activation in carcinogenesis, we investigated the potential ability of C3G to inhibit DMBA-TPA-induced skin papillomas in animal skin model, suppress proliferation of tumor cells, suppress tumor xenograft growth and metastasis in nude mice, down-regulate NF- κ B, AP-1, and MAPK activities, down-regulate the expression of COX-2 and TNF α , and scavenge ROS generated in intact cells. The results of this investigation provide new insights into the mechanisms by which a natural antioxidant may control the production of ROS-induced activation of molecular signals involved in the initiation, promotion, and progression of cancer.

MATERIALS AND METHODS

Reagents—Eagle's minimal essential medium was purchased from Whittaker Biosciences (Walkersville, MD). FBS, gentamicin, and L-glutamine were from Invitrogen. Luciferase assay kit was obtained from Promega (Madison, WI). PhosphoPlus MAPK antibody kits were purchased from New England Biolabs (Beverly, MA). Carboxymethyl dichlorofluorescein diacetate and dihydroethidium were obtained from Molecular Probes (Eugene, OR).

Cell Culture—The mouse JB6 cell line, which was stably transfected with an AP-1, NF- κ B, COX-2, or TNF α luciferase reporter plasmid (18, 29, 30), was cultured in Eagle's minimal essential medium containing 5% FBS, 2 mM L-glutamine, and 50 μ g of gentamicin/ml. Human lung carcinoma cells, A549, were cultured in Dulbecco's modified Eagle's medium containing 10% FBS. The cells were grown at 37 °C in a 5% CO₂ atmosphere.

Isolation of C3G from Blackberries—High performance liquid chromatography was used to separate and isolate C3G from blackberry fruit tissue. The detailed method for preparation of C3G has been described elsewhere (8). Briefly, fruit samples were extracted twice with 80% methanol and 0.01% HCl in a Polytron™ homogenizer for 1 min. The concentrated extract was dissolved in acidified water (0.01% HCl) and then passed through a C₁₈ Sep-Pak™ cartridge. C3G and other anthocyanins were adsorbed onto the column and then recovered from the cartridge with acidified (0.01% HCl) methanol. The methanol extract was passed through a 0.45- μ m membrane filter and further separated by a Waters Corp. high performance liquid chromatography system coupled with a photodiode array detector. The C3G-containing fraction was collected, lyophilized, and stored at –80 °C for later use. Isolation of C3G as described by this method was 99% pure.

Assay of Total Antioxidant Capacity—The total antioxidant capacity of C3G was determined using an ABTS (2,2'-azodiethylbenzthiazoline sulfonate) test set (Randox Laboratories Ltd., UK). The principle of the assay depends on production of the radical cation ABTS⁺ in incubation medium containing the substrates H₂O₂ and peroxidase. ABTS⁺ has a

blue-green color, which can be detected at 600 nm. The assays were calibrated against standards and expressed as micromoles per liter.

Cellular O₂⁻ and H₂O₂ Assay—Dihydroethidium and carboxymethyl dichlorofluorescein diacetate (CM-DCFDA) are specific dyes used for staining O₂⁻ and H₂O₂ produced by intact cells (31, 32). JB6 cells (2 × 10⁴/well) were seeded onto a glass coverslip in the bottom of a well of a 24-well plate for 24 h. The cells were pretreated with or without C3G for 30 min and exposed to UVB radiation (4 kJ/m²). At the end of the stimulation, dihydroethidium or CM-DCFDA were added at a final concentration of 5 μ M for 30 min. After the incubation, the cells were washed with phosphate-buffered saline and mounted on coverslips. A Zeiss LSM 510 microscope was used to obtain images. Scale bars were generated and inserted by using LSM software.

Assay of AP-1, NF- κ B, COX-2, and TNF α Transcription/Promoter Activity—A confluent monolayer of JB6 cells, which contained an AP-1, NF- κ B, COX-2, or TNF α luciferase-reporter plasmid, was trypsinized, and 5 × 10⁴ viable cells were seeded in each well of a 24-well plate (18, 29, 30). The cells were then pretreated with C3G for 1 h followed by exposure to TPA (20 ng/ml) or UVB radiation (4 kJ/m²) for 24 h. Then, the effects on AP-1, NF- κ B, COX-2, and TNF α induction/expression were monitored. Luciferase activity was measured using the luciferase assay kit obtained from Promega as described previously (18).

Western Blot and Protein Kinase Phosphorylation Assay—Immunoblots for phosphorylation or expression of ERKs, JNKs, p38 kinase, MEK4, and COX-2 proteins were carried out as described in the protocol from New England Biolabs, using the specific antibodies against phosphorylated sites of ERKs, JNKs, p38 kinase, and MKK4. Anti-actin antibody or non-phospho-specific antibodies provided in each assay kit were used to normalize the phosphorylation assay by using the same transferred membrane blot.

Animals and Two-stage Skin Carcinogenesis—Founder stocks for the mice (C57BL/6 crossed with DBA2) used in this study were obtained from the University of Minnesota (7). The mice were bred and housed in the West Virginia University Animal Facility. The mice were monitored free of specific pathogens housed in plastic filter-top cages on corn cob bedding, provided autoclaved tap water and Prolab 3500 feed ad libitum. Both male and female mice (6–9 weeks old) were used in groups numbering 19 to 24. Dorsal skin of the mice was shaved. A single dose of 400 nmol of 7,12-dimethylbenz[*a*]anthracene (DMBA) dissolved in 300 μ l of acetone was applied. Two weeks following initiation, the mice (except the negative control group) were promoted by dermal exposure to 17 nmol of TPA in 350 μ l of acetone twice a week for 21 weeks. For the C3G-treated group, the dorsal skin was pretreated topically with C3G (3.5 μ M/mouse) 30 min before each application of TPA. The negative control group was treated with acetone only. The incidence of papillomas was detected by palpation, and the number of papillomas appearing on each mouse was recorded once a week. At the end of the experiment, all the animals were sacrificed by intraperitoneal injection of pentobarbital (6.5 mg/mouse). For histopathology, the largest tumors were removed and fixed in freshly prepared 4% paraformaldehyde followed by paraffin embedding and subjected to pathologic evaluation.

Anchorage-independent Transformation Assay—The inhibitory effects of C3G on TPA-induced cell transformation were investigated in JB6 cells. Cells (1 × 10⁴) were suspended in 2 ml of 0.38% agar medium over 3 ml of 0.5% agar medium containing 10% FBS, 20 ng/ml TPA with or without C3G (5–80 μ M). The cultures were maintained in a 37 °C, 5% CO₂ incubator for 14 days, and the anchorage-independent colonies were scored by a computerized image analyzer.

Mouse Model Study for Tumor Xenograft Growth and Metastasis—Male nu/nu homozygous nude mice (CrI: NU-Foxn1tm, 8 weeks old)

purchased from Charles River Laboratories Inc. (Wilmington, MA). The mice were grouped in 10 mice per group and housed in autoclaved plastic filter-top cages and were provided with autoclaved tap water and Prolab 3500 feed ad libitum. Human lung carcinoma cells, A549, were harvested from tissue culture and subcutaneously injected (2×10^6 cells/flank) in both the right and left flanks of each mouse to initiate tumor growth. Two days after cell implantation, the mice were treated intraperitoneal with either PBS or C3G dissolved in PBS (9.5 mg/kg, 3 times/week). Once tumor xenografts started growing, their sizes were determined by measuring tumor size with calipers twice weekly in two dimensions throughout the study. The tumor volume was calculated by the formula, $0.5236 \times L1 \times (L2)^2$, where L1 is the long diameter and L2 is the short diameter. The tumor volume (mm^3) is represented as the mean of 10 mice in each group.

Transwell Cell Migration Assay—The assay was performed according to the methods described previously (31). The cells were serum-starved overnight, and the Transwells were coated with enhanced chemiluminescence cell attachment matrix (Upstate Biotechnology) at $20 \mu\text{g}/\text{ml}$. The top chambers of the Transwells were loaded with 0.2 ml of cells (4×10^5 cells/ml) in serum-free media, and the bottom chambers contained 0.6 ml of Dulbecco's modified Eagle's medium with 0.5% FCS. The cells were incubated in Transwells at 37°C in 5% CO_2 in the presence or absence of C3G for 12 h. Migrating cells were fixed and stained with 0.1% crystal violet, followed by dye elution. The microplate reader was used to measure the optical density of the eluted solutions to determine the migration values.

Wound Healing Assay—The wound healing assays were conducted according to the methods described previously (32). A549 cells were grown on coverslips to 100% confluent monolayer and then scratched to form a $100\text{-}\mu\text{m}$ "wound" using sterile pipette tips. The cells were then cultured in the presence or absence of C3G in serum-free media for 12 h and fixed on coverslips with 4% formalin. The images were recorded using an Olympus photomicroscope.

Cell Invasion Assay—The cell invasion assays were performed according to the methods described previously (32). A549 cells were cultured in serum-free media overnight. The cells (5×10^4 cells) were loaded on pre-coated Matrigel 24-well invasion chambers (BD Biosciences) in the presence or absence of C3G. Then 0.5 ml of 5% fetal calf serum medium was added to the wells of the plate to serve as the chemoattractant for the cells. The Matrigel invasion chambers were incubated for 18 h. The invading cells were fixed with 10% formalin, stained with Harris modified hematoxylin (Fisher), and analyzed according to manufacturer's instructions.

Statistics—Data presented are the means \pm S.E. of n assays as noted in the figure legends. Significant differences were determined using the Student's t test. Significance was set at $p \leq 0.05$.

RESULTS

Total Antioxidant Capacity of C3G—ROS have been known to be associated with many diseases. ROS are associated not only with initiation, but also with promotion and progression in the multistage carcinogenesis mode (33, 34). In light of the important role of ROS in tumor promoter-induced AP-1 activation, transformation, and progression, we measured the total antioxidant capacity of C3G using the Radox reagent set. As shown in Fig. 1A, C3G displayed a stronger antioxidant activity than that of ascorbic acid over the same concentration range, suggesting that C3G can effectively scavenge ROS.

Scavenging of H_2O_2 and O_2^- Generation by C3G—To confirm the ROS-scavenging activity of C3G, the effect of C3G on UVB-induced

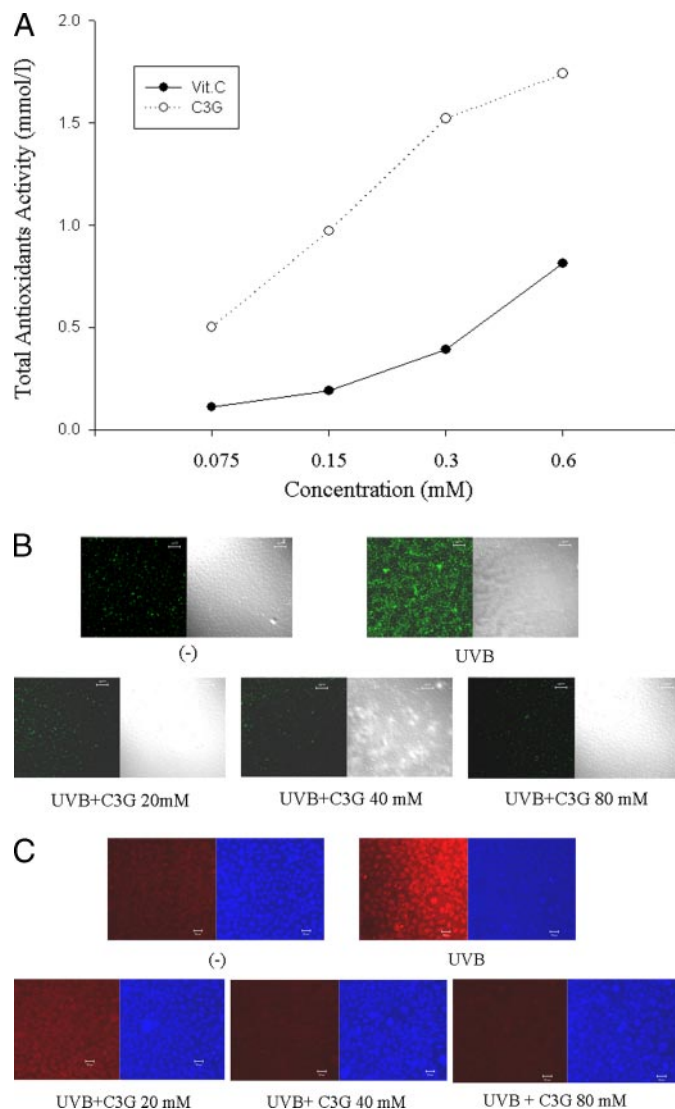


FIGURE 1. A, total antioxidant capacity of C3G. The total antioxidant capacity of C3G and ascorbic acid was determined as described under "Materials and Methods." The results were calculated as total antioxidant capacity and presented as mmol/l. B and C, confocal micrograph of inhibitory effect of C3G on UVB-induced O_2^- and H_2O_2 generation. JB6 cells were pretreated with C3G at indicated concentration and then exposed to UVB. After staining by dihydroethidium or CM-DCFDA, the images were captured with a laser scanning confocal microscope. The bright greenish areas in the cells represent oxidized CM- H_2 -DCFDA, and the bright reddish spots represent oxidized dihydroethidium showing the intracellular localization of H_2O_2 (B) and O_2^- (C), respectively.

H_2O_2 and O_2^- generated in intact cells was tested. H_2O_2 and O_2^- generation was analyzed using intracellular staining by CM- H_2 -DCFDA and dihydroethidium. CM- H_2 -DCFDA is a specific fluorescent dye for H_2O_2 , and dihydroethidium is specific for O_2^- . JB6 cells were pretreated with or without C3G for 30 min and then exposed to UVB ($4 \text{ kJ}/\text{m}^2$). The generation of H_2O_2 and O_2^- was monitored by confocal microscopy. As shown in Fig. 1 (B and C), the generation of H_2O_2 and O_2^- by UVB was completely inhibited by addition of C3G at $20 \mu\text{M}$ and $40 \mu\text{M}$, respectively.

Inhibition of AP-1, NF- κ B, COX-2, and TNF α Activation/Expression by C3G—Previous studies have shown that AP-1, NF- κ B, COX-2, and TNF α play an important role in carcinogenesis (7, 20, 21, 28). We tested the effects of C3G on UVB- and TPA-induced transactivation of AP-1 and NF- κ B, and expression of COX-2 and TNF α using a reporter gene assay in JB6 cells. The results indicated that pretreatment of the cells with various concentrations of C3G produced a dose-dependent

Chemopreventive and Chemotherapeutic Effects of C3G

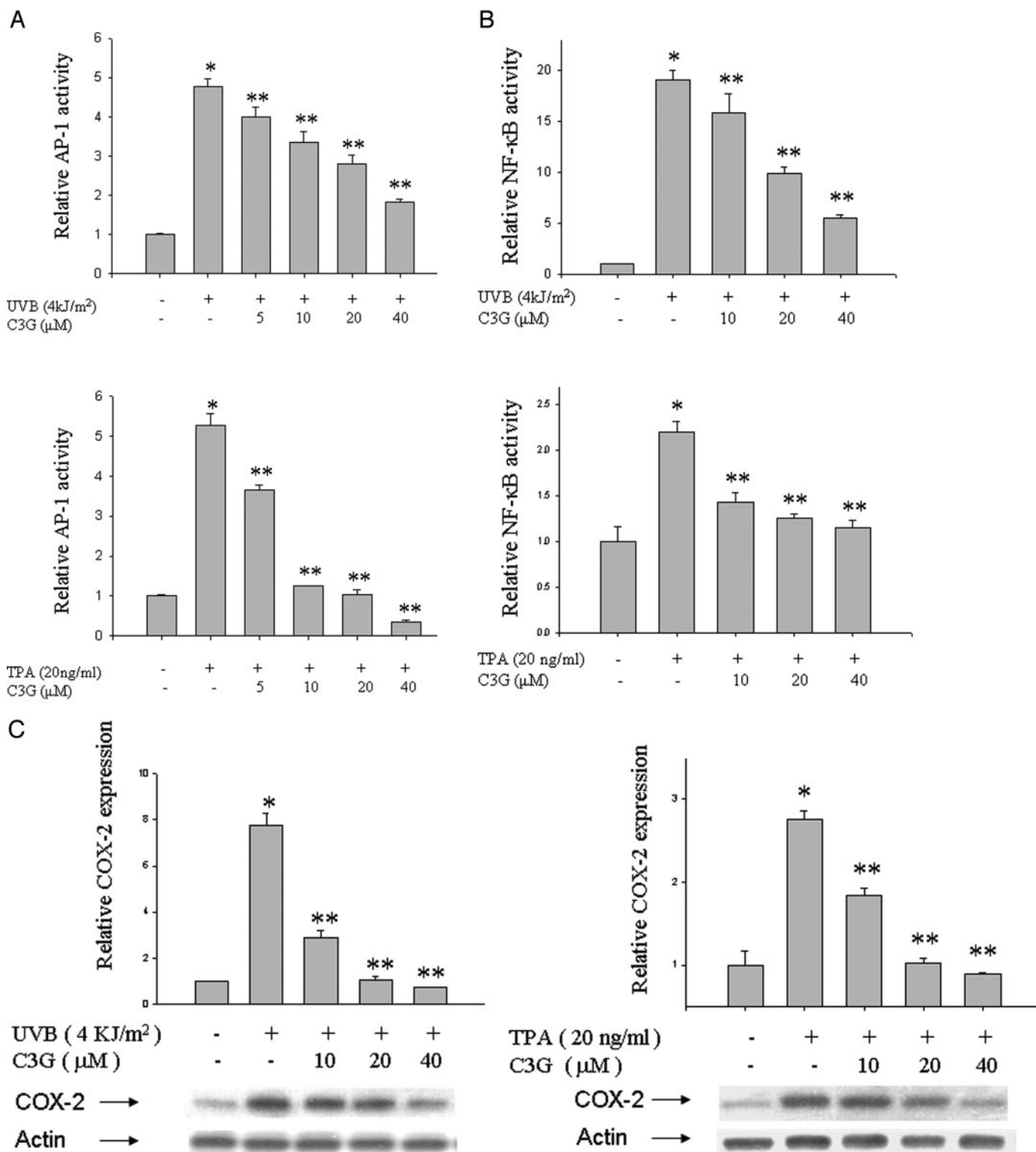


FIGURE 2. Effects of C3G on UVB- and TPA-induced AP-1, NF-κB, COX-2, TNFα, and MAPK activation/expression. The JB6 cells, which were stably transfected with the AP-1, NF-κB, COX-2, or TNFα luciferase reporter plasmid, were pretreated with C3G for 1 h followed by exposure with TPA (20 ng/ml) or UVB radiation (4 kJ/m²) for 24 h. The relative AP-1 (A) and NF-κB (B) activity, and the relative COX-2 (C) and TNFα expression (D) were measured by the luciferase assay. Results, presented as relative activity/expression compared with untreated control cells, are given as means ± S.E. from three assay wells. The experiment was repeated three times. *, significant increase from untreated negative control. **, significant decrease from the positive control. The effect of C3G on COX-2 expression was also confirmed by Western blot assay (lower panel of C).

decrease in AP-1, NF-κB, COX-2, and TNFα activity/expression induced by either UVB irradiation or TPA (Fig. 2, A–D). The induction of COX-2 expression was confirmed by Western blot analysis (Fig. 2C, bottom panel). The inhibitory actions of C3G were not caused by cyto-

toxicity, because the concentration range that inhibited AP-1, NF-κB, COX-2, and TNFα activity/expression did not affect cell proliferation as measured by the electric cell-substrate impedance sensor assay (data not shown).

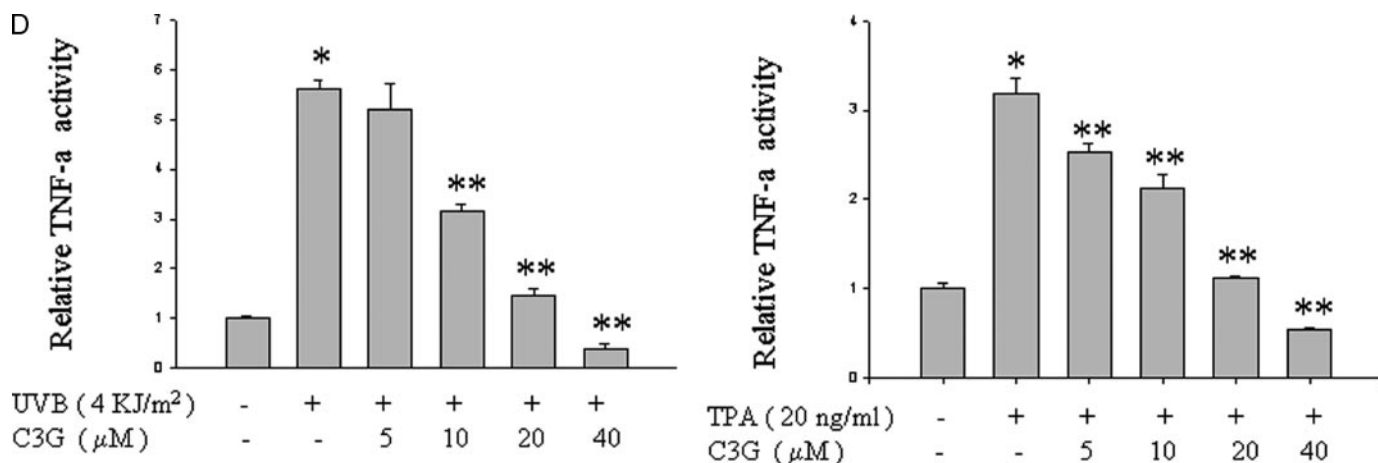


FIGURE 2.—continued

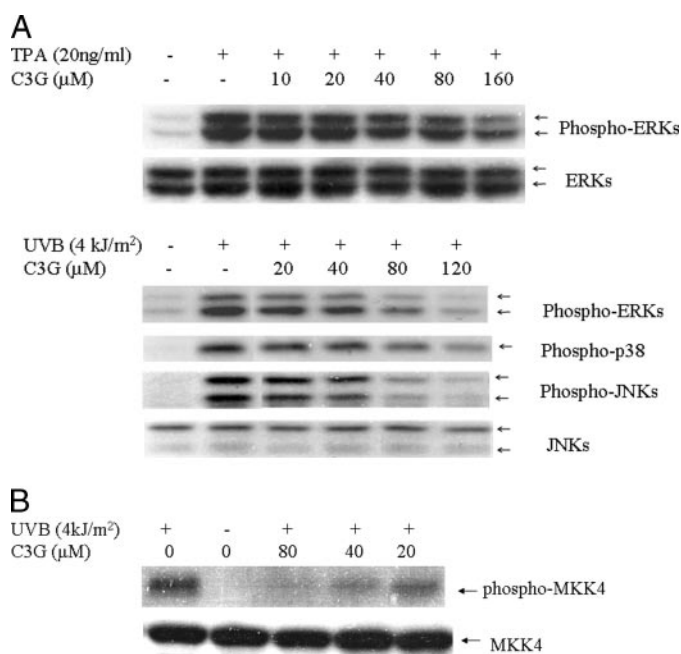


FIGURE 3. **Effect of C3G on MAPK and MKK4 activation.** JB6 cells were treated as described under "Materials and Methods." MAPKs (A) and its upstream regulator MKK4 (B) activation were analyzed by Western blot with phospho-specific antibodies against phosphorylated sites. One representative blot of three or four experiments is shown.

C3G Blocks UVB- and TPA-induced p38, ERK, and JNK Phosphorylation—Because C3G showed an inhibitory effect on AP-1, NF- κ B, COX-2, and TNF α activity/expression, we further investigated the effects of C3G on MAPK pathways. MAPK pathways, including ERK, JNK, and p38 kinase, are involved in up-regulation of AP-1 and NF- κ B activity and subsequent expression of TNF α and COX-2 by increasing the abundance of the components and/or altering the phosphorylation of their subunits (35, 36). The results indicated that C3G suppressed UVB- and TPA-induced phosphorylation of p38, ERK, and JNK (Fig. 3A), as well as the upstream regulator, MKK4 (Fig. 3B), in a dose-dependent manner. These results suggest that the mechanism by which C3G inhibits AP-1 transactivation may involve early inhibition of ERK, JNK, and p38 signaling cascades.

C3G Inhibits TPA-induced JB6 Cell Transformation—Earlier studies have indicated that AP-1 and/or NF- κ B activation is required in neo-

plastic transformation and tumorigenesis in JB6 cells (19, 20). We thus tested the effect of C3G on TPA-induced cell transformation using the soft agar assay. The result is shown in Fig. 4A. TPA-induced cell transformation was significantly inhibited by C3G at the concentration range from 10 to 40 μ M. At the concentration of 80 μ M C3G, the TPA-induced transformation was completely abolished.

Inhibition of Papillomagenesis and Malignant Transformation by C3G—To further study the antitumorigenic activity of C3G *in vivo*, we evaluated the effect of C3G on the two-stage mouse skin tumor model in which DMBA was used as initiator and TPA as promoter (37, 38). Fourteen days following DMBA initiation, the dorsal skin of the mice was exposed to TPA in the presence or absence of C3G three times per week to cause promotion. The results show that treatment of the animals with C3G decreased the number of tumors per mouse at all exposure times (Fig. 4B). Significant differences were observed 17 weeks after TPA promotion. The maximum number of papillomas after 20 weeks of TPA exposure in the C3G-treated mice was 1.59 ± 0.65 per mouse compared with 3.57 ± 1.06 papillomas per mouse in the positive control group, indicating a greater than 53% inhibition of papillomagenesis by C3G. In addition to the difference in the numbers of tumors, the size of tumors was smaller in the C3G-treated group. Two representative mice from each group showing the greatest number of papillomas are shown in Fig. 4C. Tumors in the positive control group grew rapidly and were well vascularized, whereas tumors in the C3G-treated group appeared growth-arrested and desiccated. After 22 weeks, there were four tumors greater than 4–5 mm in diameter in the TPA-treated group, whereas no large tumors were found in the C3G plus TPA-treated group. Histological analysis indicated that those large tumors were squamous cell carcinomas (data not shown). These data suggest that C3G plays an important role in preventing malignant conversion.

Effect of C3G on Proliferation of Human Lung Cancer Cells in Vitro—To further investigate the antitumor activity of C3G, the effects of C3G on proliferation of A549 cells, a human lung carcinoma cell line, were evaluated by using an electric cell-substrate impedance sensor assay. As shown in Fig. 5A, C3G dramatically inhibited proliferation of A549 in a dose-dependent manner. At the concentration of 40 μ M, the growth of tumor cells was completely blocked.

Inhibitory Effect of C3G on Tumor Growth in Mice—We further tested the *in vivo* effect of C3G on xenograft growth of A549 cells in athymic male nude mice. A549 cells were injected subcutaneously in both right and left flanks of each mouse to initiate tumor growth. Ani-

Chemopreventive and Chemotherapeutic Effects of C3G

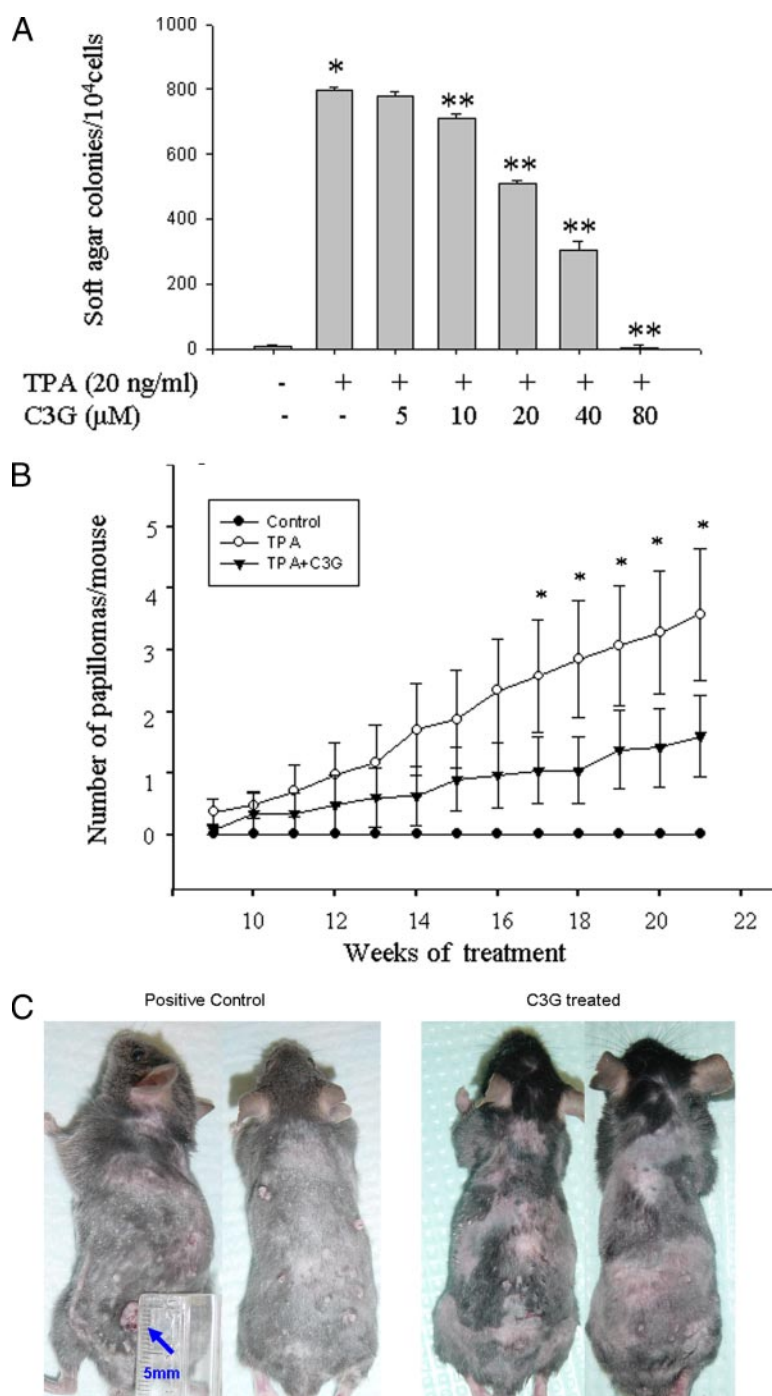


FIGURE 4. Effect of C3G on TPA-induced cell transformation and tumorigenesis in DMBA/TPA-treated mice. *A*, JB6 P⁺ cells (1×10^4) were exposed to TPA (20 μ g/ml) with or without the indicated concentrations of C3G on soft agar medium for 14 days. The cell colonies were scored by a computerized image analyzer. *, significant increase from untreated negative control. **, significant decrease from the positive control. *B*, skin tumors were generated by DMBA and TPA treatment as described under "Materials and Methods." The number of papillomas was recorded weekly. The results are presented as the mean of papillomas per mouse \pm S.E. of 21–26 mice. *, a significant difference in the number of papillomas between the positive control group and the C3G treated group ($p \leq 0.05$). *C*, external appearance of tumors. Two mice from the positive control group (*left*) and C3G-treated group (*right*) showing the greatest number of tumors are shown. The arrow indicates a tumor >5 mm in diameter.

mals were treated intraperitoneally with either PBS or C3G (9.5 mg/kg) three times per week beginning 2 days after the tumor cell implantation. As shown in Fig. 5B, tumor size showed a significant reduction in the C3G-treated group (~50% inhibition) compared with the PBS-treated control group. This result indicates that C3G treatment inhibited tumor growth in athymic nude mice.

C3G Suppresses Tumor Cell Metastasis in Mice—The effect of C3G on tumor metastasis dissemination into other organs was evaluated by macroscopic and microscopic examination of tissue sections. Pathological analysis indicated that the mice in the positive control group show a large subcutaneous tumor mass at the site of injection, and the tumors invaded through the abdominal wall and extended into the abdominal cavity, resulting in peritoneal carcinomatosis (Fig. 6A). Multiple small

tumor nodules were observed on the peritoneal surface of the abdominal wall (Fig. 6A). The tumor also was extensively involved with the mesenteric fat with malignant ascites (Fig. 6B). Tumor involvement was not only present on the surface but also within the parenchyma of organs, such as liver, kidney, pancreas, and perigastric lymph nodes (Table 1). In contrast, the C3G-treated mice showed much less tumor involvement of the abdominal cavity, although a smaller subcutaneous tumor mass at the injection site was observed. Fewer tumor nodules were observed in the abdominal cavity and the mesenteric fat. There was no tumor detected in organ parenchyma in the C3G-treated mice. Microscopically, positive control mice show a large subcutaneous tumor mass at the site of injection (Fig. 6C), whereas the injection site of the C3G-treated mice showed collections of macrophages with pig-

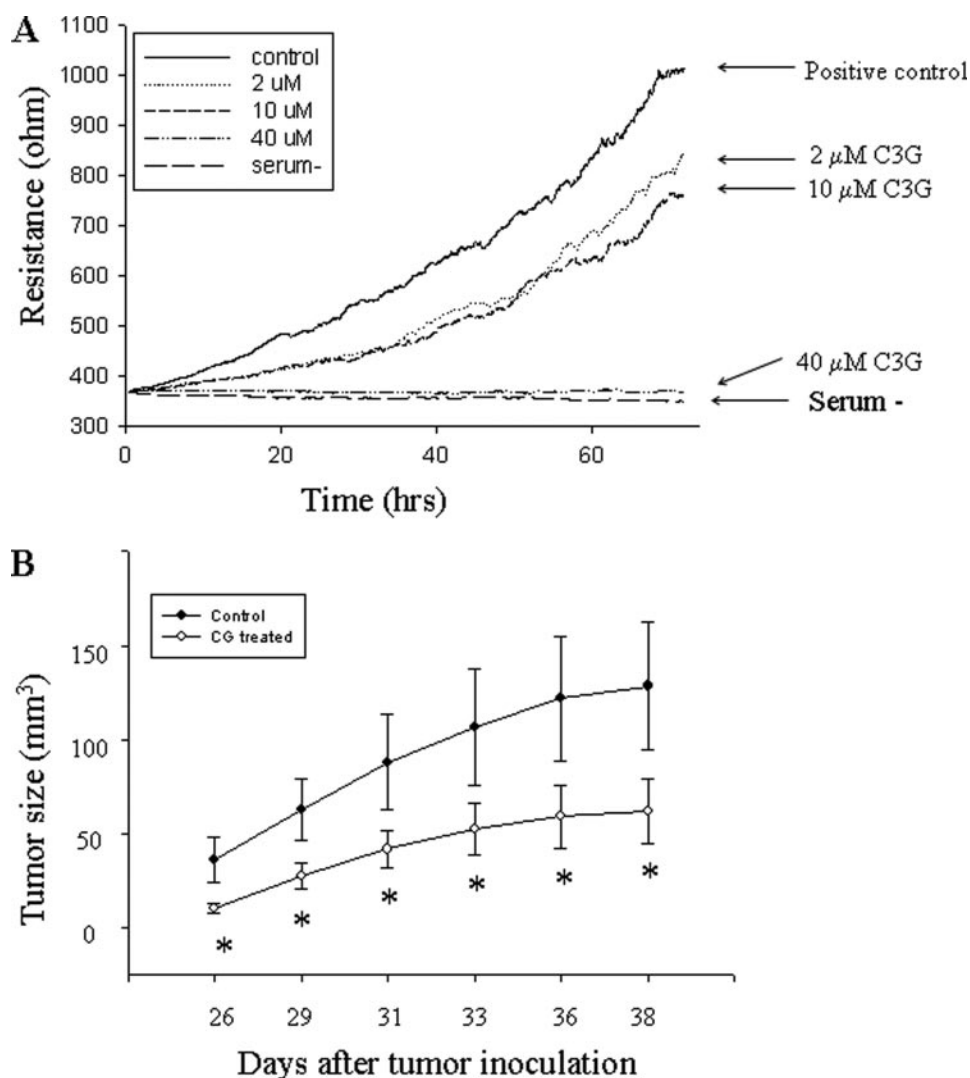


FIGURE 5. Suppression of proliferation and tumor growth of human lung carcinoma cells by C3G *in vitro* and *in vivo*. *A*, A549 cells were incubated in electrode array wells with or without C3G at the indicated concentration for 72 h. The electric cell-substrate impedance sensor resistance, indicating the cell growth, was monitored for the duration of the experiment. Data shown are representative of three independent experiments. Cells in serum-free (*Serum-*) medium were used as a negative control. *B*, male nude mice aged 8 weeks were used. A549 cells (2×10^6 /flank) were subcutaneously implanted into both right and left flanks of each mouse to initiate tumor growth. The mice were treated intraperitoneally with either PBS or C3G. Once tumor xenografts started growing, their size was measured twice weekly in two dimensions throughout the study. Tumor volume (mm^3) was calculated by the formula width² \times length \times 0.52. Each value represents the mean \pm S.E. of 10 mice. *, a significant difference from the positive control ($p < 0.02$).

ment, consistent with phagocytosis of pigment derived from the C3G compound. There were viable tumor cells in the deep skeletal muscle distant from the subcutaneous injection site. These results suggest that subcutaneous administrations of C3G not only inhibited A549 cells xenograft growth but also prevented metastasis.

Inhibitory Effects of C3G on Cancer Cell Migration and Invasion—Because cancer cell migration and invasion are the key events in metastasis, we further tested the effects of C3G on cell migration and invasion *in vitro*. Our results showed that C3G significantly blocked A549 cell migration in both wound healing assays (Fig. 7A) and Transwell assays (Fig. 7B). The potency of inhibition for cell migration was 25% at 40 μM of C3G and 70% at 80 μM of C3G in the Transwell assays (Fig. 7B). C3G was also able to inhibit cell invasion in a dose-dependent manner, 57% at 40 μM and 85% at 80 μM , as measured by Matrigel invasion assays (Fig. 7C). These results are consistent with the *in vivo* animal study, demonstrating that C3G may have the ability to inhibit cancer cell migration and invasion and prevent metastasis.

DISCUSSION

Chemoprevention, the use of drugs or natural substances to inhibit carcinogenesis, is an important and rapidly evolving aspect of cancer research that is providing a practical approach to identify potentially useful inhibitors of cancer development. Anthocyanins are a group of naturally occurring phenolic compounds related to the coloring of

plants, flowers, and fruits and recently have been reported to be as potential cancer preventive agents (10). There is increasing interest in the pharmacological activity of anthocyanins, and C3G is a major member of anthocyanins (10, 39–41). In blackberry extract, C3G represents $\sim 80\%$ of the total anthocyanins (10). Herein we report the chemopreventive and chemotherapeutic potential of C3G using *in vitro* and *in vivo* studies. The results from this study identify C3G as representing a novel compound with potent activity against a solid tumor cell growth and metastasis *in vivo*. Topical application of C3G prior to TPA application inhibits the formation of keratoacanthomas and squamous cell carcinomas in the mouse skin model. The molecular pathways involved in anticarcinogenesis by C3G were also investigated.

AP-1 and NF- κB are transcription factors that have been implicated in a wide range of cell biological events, including cell proliferation, inflammation, differentiation, metastasis, and apoptosis. Inhibition of AP-1 and NF- κB activation by a variety of agents has been shown to reduce neoplastic transformation (19). *In vivo* studies in transgenic mice indicate that AP-1 transactivation is required for tumor promotion (20). The blockade of TPA-induced cell transformation and tumorigenesis in the mouse skin model by C3G might be through the inhibition of AP-1 and NF- κB activity. Therefore, the inhibitory effects of C3G on AP-1 and NF- κB activation noted in this study suggest a potential beneficial role in preventing carcinogenesis *in vivo*.

MAPKs, including ERK, JNK, and p38 MAPK, are activated in

Chemopreventive and Chemotherapeutic Effects of C3G

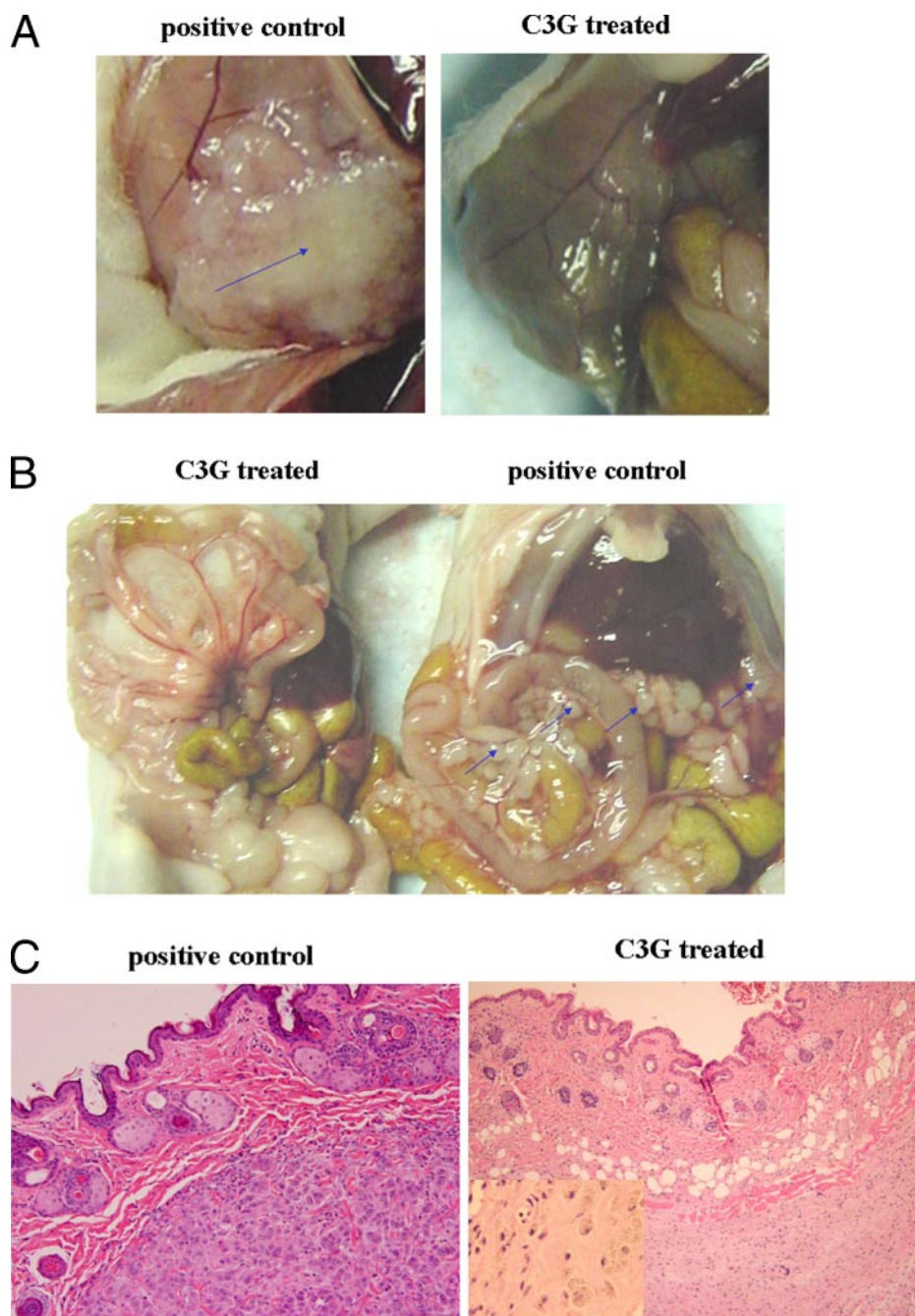


FIGURE 6. Macroscopic and microscopic findings of tumor metastases from an implanted human lung carcinoma in nude mice. *A*, in the positive control mouse, the tumor invaded through the abdominal wall and extended into the abdominal cavity, resulting in peritoneal carcinomatosis (arrow on left panel). In contrast, the C3G-treated mice showed no tumor involvement at the abdominal wall (left panel). *B*, in the positive control mouse, the tumor also extensively involved the mesenteric fat with malignant ascites (arrows). *C*, sections of implanted tumor from dorsal skin of positive control mouse (left) and C3G treated mouse (right) at 5 weeks after tumor inoculation. Tumor from positive control mouse shows aggressive growth at the injection site. In contrast, tumor from C3G-treated mouse shows less aggressive growth, and the injection site shows a collection of macrophages with pigment at a higher magnification (right bottom panel) consistent with the phagocytosed pigment derived from the C3G compound. There are viable tumor cells in the deep skeletal muscle distant from the subcutaneous injection site.

TABLE 1
Inhibitory effect of C3G on metastasis

Treatment	Number of mice	
	Peritoneal metastasis	Other parenchyma organs (liver, kidney, pancreas) metastasis
PBS	8 (80) ^a	4 (40)
C3G	2 (20)	0

^a Numbers in parentheses are percent.

response to environmental stresses and growth factors. Studies indicate that ERK, JNK, and p38 kinase are key molecules activated in response to oxidant injury. Both UVB and TPA can induce ROS generation in the cells (36, 42–44). AP-1 is a downstream target of these three MAPKs. We found that C3G could scavenge UVB-induced ROS in JB6 cells and inhibit UVB- and TPA-induced phosphorylation of ERK, JNK, and p38 kinase. These observations suggest

that these inhibitory effects on AP-1 and MAPK activation with C3G may be due to its antioxidant properties.

Angiogenesis is essential for tumor growth *in vivo* (45). Angiogenesis is a complex process where several proteins and enzymatic pathways converge. COX-2 contributes to the regulation of angiogenesis by various genes, including platelet-derived growth factor and transforming growth factor- β (46). Overexpression of COX-2 is common in non-small cell lung cancer and seems to be associated with tumor progression, invasion, and metastasis (47). Several *in vivo* studies have already shown that COX-2-specific inhibitors (celecoxib and rofecoxib) have antitumor activity (27, 48). The inhibitory effect of C3G on COX-2 expression may contribute to the suppression of human lung carcinoma growth.

Tumor invasion and metastasis are multistep and complex processes that include cell division and proliferation, proteolytic digestion of the

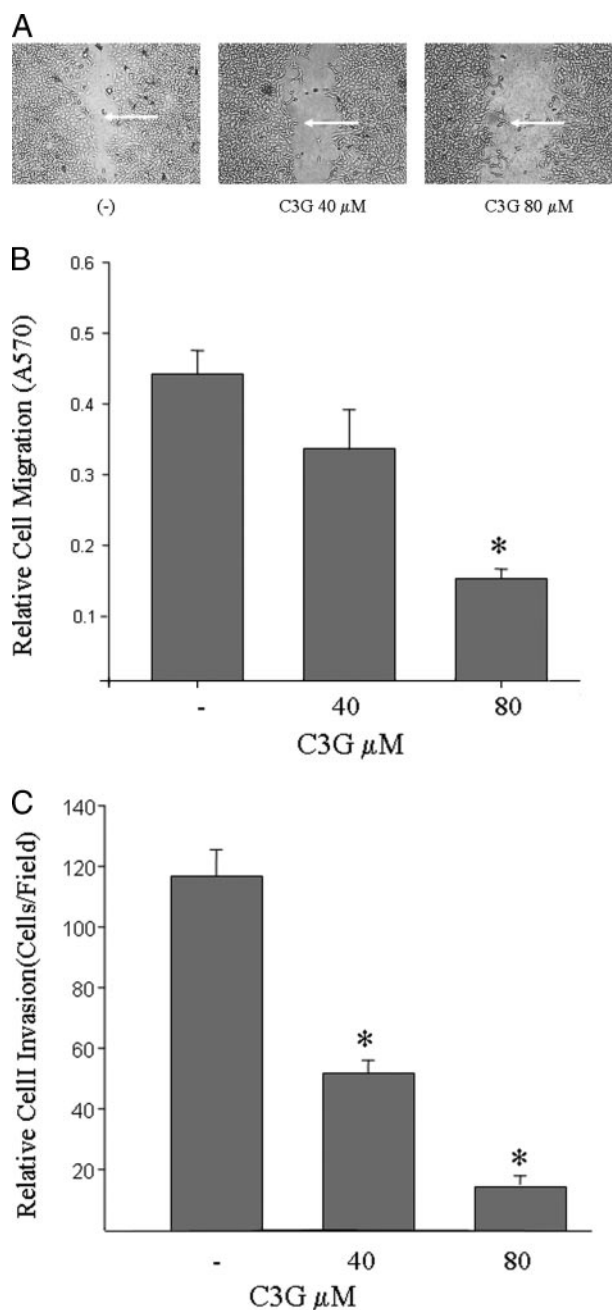


FIGURE 7. Effects of C3G on the migration and invasion of A549 cells. A, photomicrographs showing A549 cells migration 8 h after initial scraping in the absence or presence of 40 μM or 80 μM of C3G. Treatment of C3G inhibited the migration of A549 cells in a dose-dependent manner. B, graphical representation of cell migration. The data are expressed as relative cell migration (means \pm S.E.). C, Matrigel analysis on the effects of C3G on A549 cell invasion and migration. The mean values in B and C were obtained from three independent experiments. *, a significant different from the positive control group $p < 0.01$.

extracellular matrix, cell migration through the basement membranes to reach the circulatory system, and the remigration and growth of tumors at metastatic sites (50–52). AP-1 and NF- κ B are reported to up-regulate tumor cell invasion and migration through the transcriptional regulation of matrix metalloproteinase-9 and uPA (17, 18).

Activation of the MAPK pathway is a frequent event in tumorigenesis. MAPKs have been implicated in cell migration, proteinase induction, apoptosis, and angiogenesis, *i.e.* events that are essential for successful completion of metastasis (53). Recent studies have

demonstrated that MAPKs, including JNK, p38, and ERK, play crucial roles in cell migration. JNK, for example, regulates cell migration by phosphorylating paxillin, Jun, and microtubule-associated proteins. Studies of p38 show that this MAPK modulates migration by phosphorylating MAPK-activated protein kinase 2/3, which appears to be important for directionality of migration. ERK governs cell movement by phosphorylating myosin light chain kinase, calpain, or focal adhesion kinase. Therefore, the different kinases in the MAPK family all seem able to regulate cell migration but by distinct mechanisms (49, 54). Thus, the inhibitory effects of C3G on AP-1, MAPK, NF- κ B, and COX-2 may contribute to the suppression of tumor cell growth and metastasis in nude mice.

In conclusion, we have demonstrated that the phytochemical C3G exhibits chemoprevention and chemotherapeutic activities in experimental animals, possibly by interfering with signal transduction molecular, including AP-1, MAPK, NF- κ B, COX-2, and TNF α , through its ROS scavenger capacity. These data suggest that C3G may function as a potential anticancer agent with little cytotoxicity to normal tissue. Thus, C3G merits further investigation as a cancer therapeutic and preventive agent in humans. These studies establish a promising area of investigation in understanding the molecular mechanisms responsible for the beneficial effects of phytochemicals on human health.

Acknowledgment—We thank Dr. Peilin Zhang for expert assistance with pathology.

REFERENCES

- Ross, J. A., and Kasum, C. M. (2002) *Annu. Rev. Nutr.* **22**, 19–34
- Gupta, S., and Mukhtar, H. (2001) *Skin Pharmacol. Appl. Skin Physiol.* **14**, 373–385
- Surh, Y. J. (2003) *Nat. Rev. Cancer* **3**, 768–780
- American Cancer Society Advisory Committee on Diet, Nutrition, and Cancer Prevention (1996) *CA Cancer J. Clin.* **46**, 325–341
- Nishino, H., Murakoshi, M., Mou, X. Y., Wada, S., Masuda, M., Ohsaka, Y., Satomi, Y., and Jinno, K. (2005) *Oncology* **69**, 38–40
- Lu, Y. P., Lou, Y. R., Xie, J. G., Peng, Q. Y., Liao, J., Yang, C. S., Huang, M. T., and Conney, A. H. (2002) *Proc. Natl. Acad. Sci. U. S. A.* **99**, 12455–12460
- Ding, M., Lu, Y., Bowman, L., Huang, C., Leonard, S., Wang, L., Vallyathan, V., Castranova, V., and Shi, X. L. (2004) *J. Biol. Chem.* **279**, 10670–10676
- Zheng, W., and Wang, S. Y. (2003) *J. Agric. Food Chem.* **51**, 502–509
- Bagchi, D., Sen, C. K., Bagchi, M., and Atala, M. (2004) *Biochemistry (Moscow)* **69**, 75–80
- Hou, D. X. (2003) *Curr. Mol. Med.* **2**, 149–159
- Kundu, J. K., and Surh, Y. J. (2004) *Mutat. Res.* **2**, 555–565
- Dannenberg, A. J., and Subbaramaiah, K. (2003) *Cancer Cell* **4**, 431–436
- Moore, R. J., Owens, D. M., Stamp, G., Arnott, C., Burke, F., East, N., Holdsworth, H., Turner, L., Rollins, B., Pasparakis, M., Kollias, G., and Balkwill, F. (1999) *Nat. Med.* **5**, 828–831
- Afaq, F., Ahmad, N., and Mukhtar, H. (2003) *Oncogene* **22**, 9254–9264
- Adler, V., Pincus, M. R., Polotskaya, A., Montano, X., Friedman, F. K., and Ronai, Z. (1996) *J. Biol. Chem.* **271**, 23304–23309
- Lamb, R. F., Hennigan, R. F., Turnbull, K., Katsanakis, K. D., MacKenzie, E. D., Birnie, G. D., and Ozanne, B. W. (1997) *Mol. Cell. Biol.* **17**, 963–976
- Chung, T. W., Moon, S. K., Chang, Y. C., Ko, J. H., Lee, Y. C., Cho, G., Kim, S. H., Kim, J. G., and Kim, C. H. (2004) *FASEB J.* **18**, 1670–1681
- Sliva, D. (2004) *Curr. Cancer Drug Targets* **4**, 327–336
- Li, J. J., Westergaard, C., Ghosh, P., and Colburn, N. H. (1997) *Cancer Res.* **57**, 3569–3576
- Young, M. R., Li, J. J., Rincon, M., Flavell, R. A., Sathyanarayana, B. K., Hunziker, R., and Colburn, N. H. (1999) *Proc. Natl. Acad. Sci. U. S. A.* **96**, 9827–9832
- Sturm, J. W., Magdeburg, R., Berger, K., Petrich, B., Samel, S., Bonninghoff, R., Keese, M., Hafner, M., and Post, S. (2003) *Int. J. Cancer.* **107**, 11–21
- Dannenberg, A. J., Altorki, N. K., Boyle, J. O., Dang, C., Howe, L. R., Weksler, B. B., and Subbaramaiah, K. (2001) *Lancet Oncol.* **9**, 544–551
- Singh, B., Berry, J. A., Shoher, A., Ramakrishnan, V., and Lucci, A. (2005) *Int. J. Oncol.* **5**, 1393–1399
- Reddy, B. S., Maruyama, H., and Kelloff, G. (1987) *Cancer Res.* **47**, 5340–5346
- Castonguay, A., and Rioux, N. (1997) *Carcinogenesis* **18**, 491–496
- Rigas, B., and Kashfi, K. (2005) *J. Pharmacol. Exp. Ther.* **314**, 1–8

Chemopreventive and Chemotherapeutic Effects of C3G

27. Spano, J. P., Chouahnia, K., and Morere, J. F. (2004) *Bull. Cancer* **91**, 109–112
28. Aggarwal, B. B., Kumar, A., Bharti, A. C. *Anticancer Res.* (2003) **23**, 363–398
29. Ma, Q., Kinneer, K., Ye, J., and Chen, B. J. (2003) *Mol. Pharmacol.* **64**, 211–219
30. Subbaramaiah, K., Cole, P. A., and Dannenberg, A. J. (2002) *Cancer Res.* **62**, 2522–2530
31. Zamzami, N., Marchetti, P., Castedo, M., Decaudin, D., Macho, A., Hirsch, T., Susin, S. A., Petit, P. X., Mignotte, B., and Kroemer, G. (1995) *J. Exp. Med.* **182**, 367–377
32. Qian, Y., Luo, J., Leonard, S. S., Harris, G. K., Millecchia, L., Flynn, D. C., and Shi, X. (2003) *J. Biol. Chem.* **278**, 16189–16197
33. Seifried, H. E., McDonald, S. S., Anderson, D. E., Greenwald, P., and Milner, J. A. (2003) *Cancer Res.* **63**, 4295–4298
34. Benhar, M., Engelberg, D., and Levitzki, A. (2002) *EMBO Rep.* **5**, 420–425
35. Paik, J., Lee, J. Y., and Hwang, D. (2002) *Adv. Exp. Med. Biol.* **507**, 503–508
36. Karin, M. (1998) *Ann. N. Y. Acad. Sci.* **851**, 139–146
37. Balmain, A., and Pragnell, I. B. (1983) *Nature* **303**, 72–74
38. Naito, M., Chenicek, K. J., Naito, Y., and DiGiovanni, J. (1988) *Carcinogenesis* **4**, 639–645
39. Kelloff, G. J., Crowell, J. A., Steele, V. E., Lubet, R. A., Malone, W. A., Boone, C. W., Kopelovich, L., Hawk, E. T., Lieberman, R., Lawrence, J. A., Ali, I., Viner, J. L., and Sigman, C. C. (2000) *J. Nutr.* **130**, 467S–471S
40. Hou, D. X., Kai, K., Li, J. J., Lin, S., Terahara, N., Wakamatsu, M., Fujii, M., Young, M. R., and Colburn, N. (2004) *Carcinogenesis* **25**, 29–36
41. Afaq, F., Saleem, M., Krueger, C. G., Reed, J. D., and Mukhtar, H. (2005) *Int. J. Cancer* **113**, 423–433
42. Huang, C., Li, J., Ding, M., Leonard, S. S., Wang, L., Castranova, V., Vallyathan, V., and Shi, X. (2001) *J. Biol. Chem.* **276**, 40234–40240
43. Kyriakis, J. M., Banerjee, P., Nikolakaki, E., Dai, T., Rubie, E. A., Ahmad, M. F., Avruch, J., and Woodgett, J. R. (1994) *Nature* **369**, 156–160
44. Whitmarsh, A. J., and Davis, R. J. (1996) *J. Mol. Med.* **74**, 589–607
45. Weidner, N., and Folkman, J. (1996) *Important Advances in Oncology*, pp. 167–190, Lippincott-Raven, Philadelphia
46. Tsujii, M., Kawano, S., Tsuji, S., Sawaoka, H., Hori, M., and DuBois, R. N. (1998) *Cell* **93**, 705–716
47. Marrogi, A. J., Travis, W. D., Welsh, J. A., Khan, M. A., Rahim, H., Tazelaar, H., Pairolero, P., Trastek, V., Jett, J., Caporaso, N. E., Liotta, L. A., and Harris, C. C. (2000) *Clin. Cancer Res.* **6**, 4739–4744
48. Chen, T., Hwang, H., Rose, M. E., Nines, R. G., and Stone, G. D. (2006) *Cancer Res.* **66**, 2853–2859
49. Huang, C., Rajfur, Z., Borchers, C., Schaller, M. D., and Jacobson, K. (2003) *Nature* **424**, 219–223
50. Kleiner, D. E., and Stetler-Stevenson, W. G. (1999) *Cancer Chemother. Pharmacol.* **43**, 42–51
51. Lochter, A., and Bissell, M. J. (1999) *APMIS* **107**, 128–136
52. Folkman, J. (1995) *N. Engl. J. Med.* **333**, 1757–1763
53. Reddy, K. B., Nabha, S. M., and Atanaskova, N. (2003) *Cancer Metastasis Rev.* **4**, 395–403
54. Huang, C., Jacobson, K., and Schaller, M. D. (2004) *J. Cell Sci.* **117**, 4619–4628